ELSEVIER

Journal of Power Sources 85 (2000) 279–283

JOURNAL OF POWER SOURCES

www.elsevier.com/locate/jpowsour

Structural, physical and electrochemical characterisation of $LiNi_xCo_{1-x}O_2$ solid solutions

G.X. Wang *, J. Horvat, D.H. Bradhurst, H.K. Liu, S.X. Dou

Energy Storage Materials Program, Institute for Superconducting and Electronic Materials, University of Wollongong, Wollogong, NSW 2522, Australia

Received 12 July 1999; accepted 4 August 1999

Abstract

$LiNi_xCo_{1-x}O_2$ solid solutions are synthesised and their electrochemical performance as cathodes is examined in lithium cells. Through DTA/TG analysis and self-discharge tests, it is found that both the thermal stability at high temperature and the electrochemical stability in the fully-charged state for $LiNi_xCo_{1-x}O_2$ increases with increasing content of cobalt in the compound. The average operating potentials for the solid solutions are lower than those for pure $LiCoO_2$. This indicates that both cobalt and nickel take part in the redox reactions during lithium insertion and extraction. The substitution of Ni^{3+} for Co^{3+} in $LiNi_xCo_{1-x}O_2$ can improve the specific capacity, but with a small sacrifice in cycleability.

Keywords: $LiNi_xCo_{1-x}O_2$ solid solutions; Lithium-ion batteries; Magnetic susceptibility; Thermal and electrochemical stability

1. Introduction

Lithium-ion batteries are state-of-the-art power sources for modern portable electronic devices. $LiCoO_2$ and carbon are currently used, respectively, as cathode and anode materials in commercial lithium-ion batteries [1]. $LiCoO_2$ suffers several disadvantages because of its high cost, toxicity and the associated impact on the environment. The search for alternatives for $LiCoO_2$ is being pursued worldwide. Spinel $LiMn_2O_4$ is one of the alternative cathode materials for lithium-ion batteries. A tremendous amount of work has been done on this material [1–4]. Unfortunately, it is still not ready to be used in commercial production due to its short cycle-life, which is associated with the phase transformation of the spinel during the charge–discharge cycle [2–6].

$LiNiO_2$ with the isostructure of $LiCoO_2$ has shown some promise as the cathodic material for lithium-ion batteries. $LiNiO_2$ has a higher capacity (170 to 190 mA h g^{-1}) than $LiCoO_2$ (140 mA h g^{-1}). On the other hand, its thermal and electrochemical stability are not as good as $LiCoO_2$, and these features induce inferior cycleability [7–9]. Aluminium has been used to stabilize $LiNiO_2$ and the electrochemical performance of $LiNiO_2$ can be improved by the aluminium dopant effect [10–12]. For practical applications, lithium-ion batteries have to endure more than one thousand cycles. In this regard, it is still doubtful whether $LiNiO_2$ or $LiAl_xNi_{1-x}O_2$ will be able to replace $LiCoO_2$.

It might be possible, however, to substitute cobalt partially with nickel in the $LiCoO_2$ structure and still retain the excellent electrochemical performance of $LiCoO_2$. In this investigation, a series of $LiNi_xCo_{1-x}O_2$ solid solutions have been prepared and their electrochemical properties as cathodes in lithium-ion cells have been compared.

2. Experimental

$LiNi_xCo_{1-x}O_2$ solid-solutions ($x = 0$, 0.25, 0.5, 0.75, 1) were prepared by heat-treating the precursor reagents $LiOH \cdot H_2O$, NiO, and CoO (99.9%, Aldrich) at 750°C for 24 h under an oxygen flow. Before the heat treatment, the precursors were ball-milled for 8 h and then pressed into pellets. The $LiNi_xCo_{1-x}O_2$ powders were characterized by X-ray diffraction by means of a MO3XHF[22] diffractometer (MaCScience, Japan) with a curved crystal (graphite 002) diffracted beam monochromator and Cu-Kα radiation. Silicon powder was used as an internal standard to calculate the lattice parameters of the unit cell. Thermal analysis was carried out on a SETARAM (92 Model,

* Corresponding author. Fax: +61-2-215731; e-mail: gw14@uow.edu.au

0378-7753/00/$ - see front matter
PII: S0378-7753(99)00349-3

France) simultaneous DTA/TG analyser to determine the thermal stability of $LiNi_xCo_{1-x}O_2$ at high temperature.

The electrochemical performance of $LiNi_xCo_{1-x}O_2$ as cathodes in lithium cells was examined using CR2032 coin cells. The cathode was made by dispersing a mixture of 85 wt.% active materials, 12 wt.% carbon black and 3 wt.% PVDF binder in dimethyl phthalate (DMP) to form a slurry. The slurry was then spread on to aluminum foil. The electrodes were dried at 140°C under vacuum for 20 h. The electrolyte was 1 M $LiPF_6$ in a mixture of EC (ethylene carbonate) and DMC (dimethyl carbonate) (Merck KGaA, Germany). The coin cells were assembled by a hand-operated closing tool (Hohsen, Japan) in an argon filled glove-box (Unilab, Mbraun, USA) in which the oxygen and moisture were controlled to less than 1 ppm. The lithium test cells were cycled at a constant current density of 0.15 mA cm^{-2} over a voltage window of 3.0 to 4.4 V vs. Li/Li^+.

3. Results and discussion

3.1. Structural and physical properties of $LiNi_xCo_{1-x}O_2$ solid solutions

X-ray diffraction (XRD) patterns of $LiNi_xCo_{1-x}O_2$ solid-solutions are presented in Fig. 1. No impurity phase was detected by XRD analysis. This indicates that Co^{3+} and Ni^{3+} ions are compatible in the layered $R\bar{3}m$ hexagonal structure and pure-phase solid solutions were obtained. With the mixtures of Co^{3+} and Ni^{3+} in the structure, all the diffraction peaks were observed to broaden by comparison with those of pure $LiCoO_2$ and $LiNiO_2$. This suggests that there exists a microscopic stress in the basa plane, which is probably caused by the mismatch of Co^{3+} and Ni^{3+} ions due to the difference in their radii. For pure $LiCoO_2$, the (006)(102) and (108)(110) lines split clearly. With the addition of Ni^{3+}, however, these two couple of lines gradually converge. All the diffraction lines, except the (003) line, shift to lower angles with increase in Ni^{3+} content. The lattice constants were calculated using a least-squares method with 16 diffraction lines. As shown in Fig. 2, the lattice constants *a* and *c* increase with increase in Ni^{3+} content.

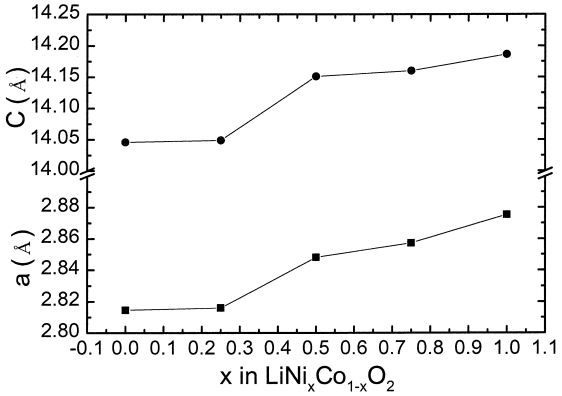

Fig. 2. Variation of lattice constants *a* and *c* in $LiNi_xCo_{1-x}O_2$.

Thermo-gravimetric analysis was performed on $LiNi_xCo_{1-x}O_2$ compounds in dry air. The samples were heated at 10°C/min up to 1000°C. The weight losses of the five $LiNi_xCo_{1-x}O_2$ samples are shown in Fig. 3. The $LiCoO_2$ was the most stable among all of the samples at high temperature. The thermal stability decreases with increase in Ni content. By contrast, $LiNiO_2$ demonstrated a greater weight loss than the other $LiNi_xCo_{1-x}O_2$ solid solutions.

The weight loss of $LiNi_xCo_{1-x}O_2$ compounds at high temperature can be attributed to the extraction of oxygen from the structure according to the following reaction:

$$(1+\delta)LiNi_xCo_{1-x}O_2 \rightarrow Li_{1-\delta}(Ni_xCo_{1-x})_{1+\delta}O_2 + \delta Li_2O + 0.5\delta O_2 \quad (1)$$

The deterioration of the thermal stability of $LiNi_xCo_{1-x}O_2$ with the addition of nickel can be associated with the

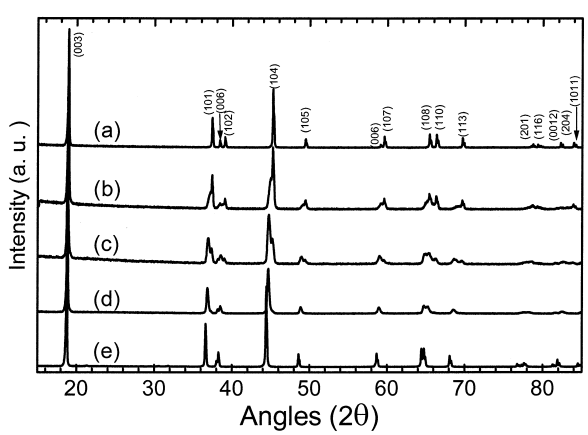

Fig. 1. X-ray diffraction patterns of $LiNi_xCo_{1-x}O_2$ solid-solutions: (a) $LiCoO_2$; (b) $LiNi_{0.25}Co_{0.75}O_2$; (c) $LiNi_{0.5}Co_{0.5}O_2$; (d) $LiNi_{0.75}Co_{0.25}O_2$; (e) $LiNiO_2$.

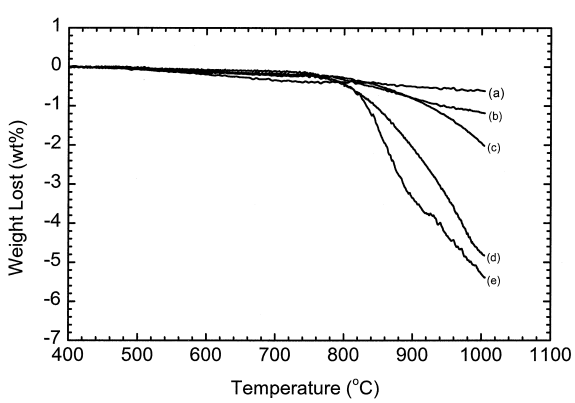

Fig. 3. Weight loss vs. temperature for $LiNi_xCo_{1-x}O_2$ solid-solutions. TGA was conducted under dry air at a rate of 10°C/min from 45 to 1000°C: (a) $LiCoO_2$; (b) $LiNi_{0.25}Co_{0.75}O_2$; (c) $LiNi_{0.5}Co_{0.5}O_2$; (d) $LiNi_{0.75}Co_{0.25}O_2$; (e) $LiNiO_2$.

binding-energy (E_{BE}) of the M–O bond. The binding-energy data for the M–O bond in $LiNi_xCo_{1-x}O_2$ crystal is not available, but can be estimated by relating the thermodynamic functions of MO_2 with Born–Haber's cyclic process. The binding-energies of CoO_2 and NiO_2 are 1067 and 1029 kJ/mol, respectively, Thus, the Co–O bond is stronger than the Ni–O bond [13]. Therefore, it is reasonable that the thermal stability of $LiNi_xCo_{1-x}O_2$ deteriorates with the addition of nickel in the structure, and that stoichiometric $LiNiO_2$ is difficult to synthesize [9].

Temperature-dependent magnetic measurements were performed on $LiNi_xCo_{1-x}O_2$ powders in a d.c. field of 1000 G using a Quantum Design Magnetometer (PPMS, USA). The temperature-dependence of the magnetic susceptibility of the $LiNi_xCo_{1-x}O_2$ solid solutions is shown in Fig. 4. The paramagnetic Curie constants, θ, are also provided. All $LiNi_xCo_{1-x}O_2$ compounds obey the Curie–Weiss law, $\chi = C/(T-\theta)$, at high temperature. $LiCoO_2$ and $LiNi_{0.25}Co_{0.75}O_2$ have a negative paramagnetic Curie constant θ, which indicates antiferromagnetic behaviour below T_c. By contrast, $LiNi_{0.5}Co_{0.5}O_2$, $LiNi_{0.75}Co_{0.25}O_2$ and pure $LiNiO_2$ compounds have a positive θ, which indicates a ferromagnetic interaction of the magnetic centres [14,15]. Both Ni^{3+} ($3d^7$, low spin) and Co^{3+} ($3d^6$, low spin) are magnetic ions. $LiNi_xCo_{1-x}O_2$ solid-solutions have a rhombohedral structure $R\bar{3}m$ in which Li^+, Ni^{3+} or Co^{3+}, and O^{2-} occupy 3a, 3b, and 6c sites, respectively. Non-magnetic lithium layers alternate with magnetic nickel, cobalt or nickel–cobalt layers. Therefore, magnetic correlation between nickel ions in $LiNiO_2$, cobalt ions in $LiCoO_2$ and nickel–cobalt ions in $LiNi_xCo_{1-x}O_2$ solid solutions are generally considered to be two-dimensional. $LiCoO_2$ normally has an ordered structure, whereas $LiNiO_2$ has a disordered structure with the nickel partially in 3a sites. The ferromagnetic anomalies for $LiNiO_2$, $LiNi_{0.75}Co_{0.25}O_2$ and $LiNi_{0.5}Co_{0.5}O_2$ are probably caused by part of the nickel or cobalt ions at 3a sites producing strong magnetic interactions of Ni (3b) [or Co (3b)] –O– Ni (3a) [or Co (3a)] –O– Ni (3b) [or Co (3b)] between different [NiO_2] or [CoO_2] layers. Accordingly, three-dimensional connections between the two-dimensional nickel layers or cobalt layers are created and introduce a three-dimensional magnetic correlation [16–18]. The ferromagnetic susceptibility for $LiNiO_2$ in this investigation is not as strong as described in Ref. [14]. This suggests that our sample has a relatively more ordered structure.

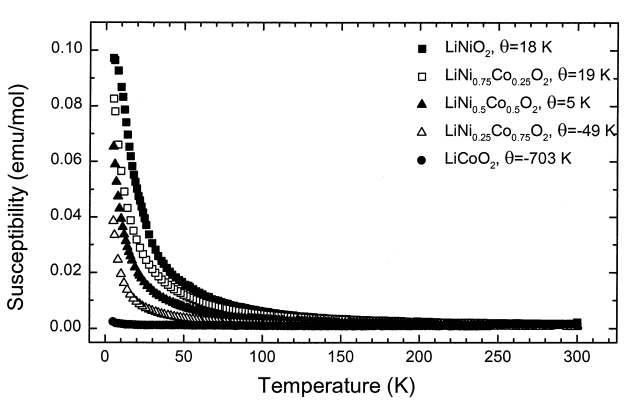

Fig. 4. Magnetic susceptibility χ vs. T for $LiNi_xCo_{1-x}O_2$ compounds.

3.2. Electrochemical performance of $LiNi_xCo_{1-x}O_2$ as cathodes in li-ion cells

$Li/LiNi_xCo_{1-x}O_2$ coin cells were fabricated to examine the electrochemical performance of $LiNi_xCo_{1-x}O_2$ solid-solutions as cathodes in lithium cells. The initial charge–discharge profiles of the $Li/LiNi_xCo_{1-x}O_2$ cells are presented in Fig. 5. The $LiCoO_2$ electrode delivered an initial discharge capacity of 141 mA h g^{-1}. On the other hand, the capacity of the $LiNiO_2$ electrode can reach 181 mA h g^{-1} in the first discharge. The initial discharge capacities for $LiNi_xCo_{1-x}O_2$ solid-solutions were between those of $LiCoO_2$ and $LiNiO_2$. During the first charge, the $LiCoO_2$ was quickly charged to 3.9–4.0 V and then followed a slope up to the cut-off voltage of 4.4 V. During the discharge, the $LiCoO_2$ electrode delivered a discharge capacity mainly in the range of 4.2 to 3.8 V. The operating potentials for $LiNi_xCo_{1-x}O_2$ ($x = 0.25$, 0.5, 0.75, 1.0) were between 4.2 and 3.6 V vs. Li/Li^+. It has been observed that all $LiNi_xCo_{1-x}O_2$ electrodes were quickly charged to 3.6–3.7 V and then followed a slope up to the cut-off voltage during the initial charging process. This behaviour was also observed during subsequent charge–discharge cycles. Three samples were tested for each composition of $LiNi_xCo_{1-x}O_2$ and the same behaviour was demonstrated as shown in Fig. 5. Therefore, we conclude that the average charge–discharge potentials of $LiNi_xCo_{1-x}O_2$ electrodes decline as nickel is added to the $LiCoO_2$ structure. The operating voltage is approximately in the order: MnO_2 ($3d^3/3d^4$) ≥ CoO_2 ($3d^5/3d^6$) > NiO_2 ($3d^6/3d^7$), which is related to the Fermi energy of the electrons in the 3d orbital [19]. The decline of the operating potential for $LiNi_xCo_{1-x}O_2$ solid-solutions means that both nickel and cobalt participate in the redox reaction during the charge–discharge process. In the initial charge–discharge cycle, approximately 15 to 35 mA h g^{-1} capacity is irreversible for the $LiNi_xCo_{1-x}O_2$ electrodes. The highest irreversible capacity of 34 mA h g^{-1} was observed for the $LiNiO_2$ electrode. For solid solutions containing cobalt in the structure, the irreversible capacity declines to 15–20 mA h g^{-1}. These irreversible capacity losses in the first cycle can be utilized to compensate for lithium consumption on the surface of the carbon anode due to the formation of the passivation film in the first charge of commercial lithium-ion batteries.

In order to determine the cycleability of $LiNi_xCo_{1-x}O_2$ electrodes, the $Li/LiNi_xCo_{1-x}O_2$ coin cells were cycled within the voltage range 3.0 to 4.4 V at a constant current density of 0.15 mA cm^{-2} for 100 cycles. The results of

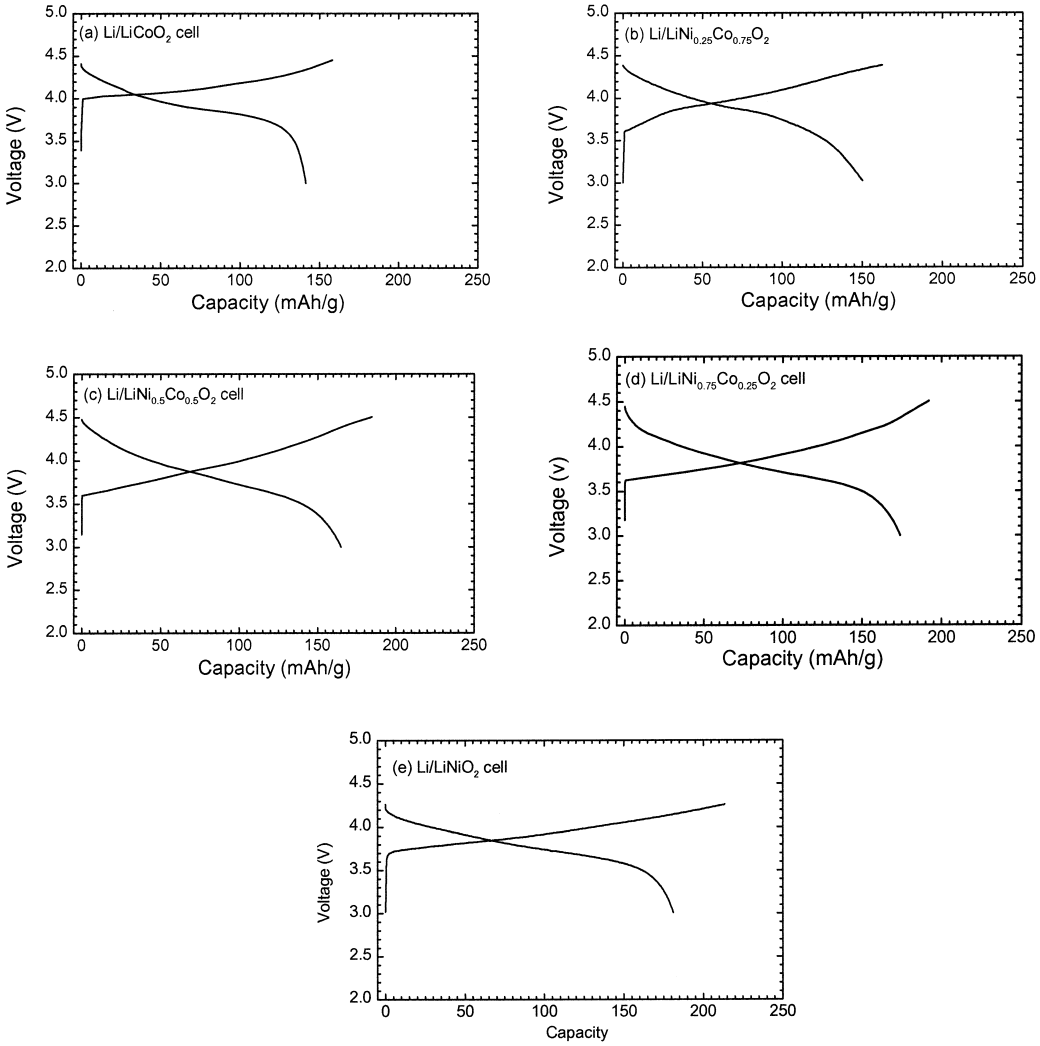

Fig. 5. First charge–discharge profiles for $Li/LiNi_xCo_{1-x}O_2$ cells. Charge and discharge current density was 0.15 mA h cm^{-2}.

the cycling tests are shown in Fig. 6. The $LiCoO_2$ electrode demonstrates an excellent cycleability compared with the $LiNiO_2$ electrode. The rechargeability for $LiNi_{0.5}Co_{0.5}O_2$ and $LiNi_{0.25}Co_{0.75}O_2$ electrodes is still good with a capacity fading rate of 0.3 and 0.18 mA h g^{-1} per cycle, respectively. In this investigation, lithium foil was used as the anode. After 100 cycles, the cells were dismantled in the glove-box. A layer of lithium powder was found on the surface of the lithium anode, which undoubtedly influenced the cycle-life of the cells. If commercial carbon is used as the anode, the results of the cycle-life test would have been expected to be better.

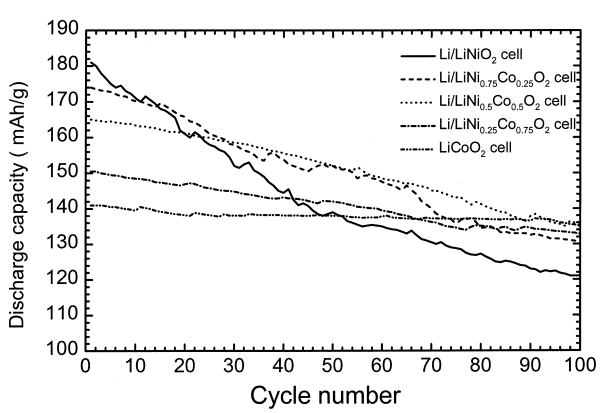

Fig. 6. Discharge capacity vs. cycle number for $Li/LiNi_xCo_{1-x}O_2$ cells.

The mechanism for the capacity fade of $LiNi_xCo_{1-x}O_2$ electrodes on cycling could be due to the following factors: (i) the structural change due to, lithium insertion/extraction causes the contraction and expansion of the unit cell, which may lead to the formation of fractures in the particles of the active materials; (ii) in the charged state, MO_2 reacts with the organic electrolyte and induces the dissolution of M ions into the solution. $LiNiO_2$ has been identified to experience several topatactic phase transformations during lithium insertion and extraction processes [20]. This phenomenon has not been observed for $LiCoO_2$. Therefore, in $LiNi_xCo_{1-x}O_2$ solid-solutions, cobalt can

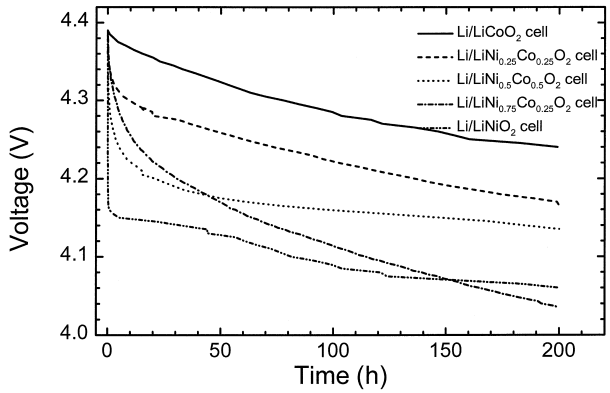

Fig. 7. Self-discharge of $Li/LiNi_xCo_{1-x}O_2$ cells in highly charged state.

stabilize the layered structure for insertion and extraction of lithium ions. The binding energy of the Co–O bond is higher than that of the Ni–O bond. The strong Co–O skeleton can contribute to the stability of $LiCoO_2$ in the charged state. In order to confirm this point of view, self-discharge tests have been performed on $Li/LiNi_xCo_{1-x}O_2$ cells. The cells were charged to 4.4 V and then the charging current was cut off. The cells were left to relax for 200 h and the decay of the cell voltage was recorded. As shown in Fig. 7, the stability of $LiNi_xCo_{1-x}O_2$ electrodes in the charged state increases with increasing amount of cobalt in the structure. The decline in the cell voltage in the charged state is probably caused by the reaction of $[Ni_xCo_{1-x}O_2]^-$ with the organic electrolyte because in the fully-charged state, nickel and cobalt are at $4+$, which is very reactive. Therefore, limiting the charging voltage (e.g., to 4.2 V vs. Li/Li^+ instead of 4.4–4.5 V) could extend the cycle-life of $LiNi_xCo_{1-x}O_2$ electrodes.

4. Conclusions

Thermogravimetric analysis and self-discharge tests show that the thermal stability and electrochemical stability of $LiNi_xCo_{1-x}O_2$ increase with increasing cobalt content in the structure. This is associated with the binding energy of the M–O bond. Measurements of the magnetic susceptibility of $LiNi_xCo_{1-x}O_2$ powders demonstrate that an ordered layered structure can be obtained by an appropriate synthesis process. The partial substitution of nickel for cobalt in the layered $LiCoO_2$ structure can improve the initial specific capacity but the cycleability deteriorates. Correspondingly, the cost and toxicity of the electrode material can be reduced. Trading-off these factors, $LiNi_{0.5}Co_{0.5}O_2$ could be a reasonable choice as a cathodic material for lithium-ion batteries.

References

[1] T. Nagaura, K. Tazawa, Prog. Batteries Sol. Cells 9 (1990) 20.
[2] A. de Kock, E. Feng, R.J. Gummow, J. Power Sources 70 (1998) 247–252.
[3] J.M. Tarascon, W.R. McKinnon, F. Coowar, T.N. Bowmer, G. Amatucci, D. Guyomard, J. Electrochem. Soc. 141 (1994) 1421.
[4] R.J. Gummow, A. de Kock, M.M. Thackeray, Solid State Ionics 69 (1994) 59–67.
[5] A.D. Robertson, S.H. Lu, W.F. Averill, W.F. Howard Jr., J. Electrochem. Soc. 144 (1997) 3500.
[6] A. Yamada, K. Miura, K. Hinokuma, M. Tanaka, J. Electrochem. Soc. 142 (1995) 2149.
[7] T. Ohzuku, A. Ueda, M. Nagayama, J. Electrochem. Soc. 140 (1993) 1862.
[8] M. Broussely, F. Perton, P. Biensan, J.M. Bodet, J. Labat, A. Lecerf, C. Delmas, A. Rongier, J.P. Pérès, J. Power Sources 54 (1995) 109–114.
[9] G.X. Wang, S. Zhong, D.H. Bradhurst, S.X. Dou, H.K. Liu, J. Power Sources 76 (1998) 141–146.
[10] T. Ohzuku, A. Ueda, M. Kouguchi, J. Electrochem. Soc. 142 (1995) 4033.
[11] Q. Zhong, U. Von Sacken, J. Power Sources 54 (1995) 221–223.
[12] G.X. Wang, S. Zhong, D.H. Bradhurst, S.X. Dou, H.K. Liu, Solid State Ionics 116 (1999) 271–277.
[13] L. Guohua, H. Ikuta, T. Uchida, M. Wakihara, J. Electrochem. Soc. 143 (1996) 178.
[14] M.E. Spahr, P. Novák, B. Schnyder, O. Haas, R. Nesper, J. Electrochem. Soc. 145 (1998) 1113.
[15] K. Hirota, Y. Nakazawa, M. Ishikawa, J. Phys. Condens. Mater. 3 (1991) 4721.
[16] A. Ott, P. Endres, V. Klein, B. Fuchs, A. Jäger, H.A. Mayer, S. Kemmler-Sack, H.-W. Praas, K. Brandt, G. Filoti, V. Kunczer, M. Rosenberg, J. Power Sources 72 (1998) 1–8.
[17] K. Yamaura, M. Takano, A. Hirano, R. Kanno, J. Solid State Chem. 127 (1996) 109.
[18] J.N. Reimers, J.R. Dahn, J.E. Greedan, C.V. Stager, G. Liu, I. Davidson, U. von Sacken, J. Solid State Chem. 102 (1993) 542.
[19] A. Ueda, T. Ohzuku, J. Electrochem. Soc. 141 (1994) 2010–2014.
[20] W. Li, J.N. Reimers, J.R. Dahn, Solid State Ionics 67 (1993) 123.